Proceedings of the 1998 U.S. DOE Hydrogen Program Review

NREL/CP-570-25315

# A POLYMER ELECTROLYTE FUEL CELL STACK FOR STATIONARY POWER GENERATION FROM HYDROGEN FUEL

Mahlon S. Wilson, Steffen Møller-Holst, Daniel M. Webb,
Christine Zawodzinski and Shimshon Gottesfeld
Materials Science and Technology Division, MS D429
Los Alamos National Laboratory, Los Alamos, NM 87545

## Abstract

Our objective is to develop and demonstrate a 4 kW, hydrogen-fueled polymer electrolyte fuel cell (PEFC) stack, based on non-machined stainless steel hardware and on membrane/electrode assemblies (MEAs) of low catalyst loadings. The stack is designed to operate at ambient pressure on the air-side and can accommodate operation at higher fuel pressures, if so required. This is to be accomplished by working jointly with a fuel cell stack manufacturer, based on a CRADA. The performance goals are 57% energy conversion efficiency hydrogen-to-electricity (DC) at a power density of 0.9 kW/liter for a stack operating at ambient inlet pressures. The cost goal is $600/kW, based on present materials costs.

## Technical Goals

Our main Tasks for FY-98 are centered on the fabrication of a 4 kW stainless steel ambient pressure Sstack. The first step in this effort is work with a single cell of the new, ambient pressure 300 $cm^2$ design, followed by the demonstration of a short, 3-5 cell stainless steel ambient pressure stack, demonstration of a 4 kW stack, and bench testing of a system which would include complete air and water management for the 4 kW stack, targeting parasitic power levels lower than 10%.

## Major Barriers to Meeting Technical Goals

An important barrier to implementation of low cost, non-machined metal hardware technology in PEFC stacks, is the potential susceptibility of the metal or alloy selected to corrosion or to surface passivation under some combination of conditions likely to occur, for a given stack design, on either cathode or anode sides. Effective water management needs to be achieved, particularly at ambient pressure. While we have previously demonstrated relatively high performance ambient pressure 8 and 12 cell stacks with 100 $cm^2$ active areas and machined graphite hardware, the new, larger (300 $cm^2$ active area) metal hardware substantially alters many subtle factors that influence cell performance. To a large extent, the system needs to be re-optimized. Development of novel stack technology requires solving a variety of engineering issues such as effective component design, stack sealing, and (lab-scale) fabrication of a significant number of stack components. We were initially delayed when critical components were delivered months after originally scheduled. Unfortunately, these components were not to specifications and were not uniformly consistent. A considerable amount of further effort has been expended in designing around and/or accommodating the deficiencies of these critical components.

## Approach/Background

The approach of this project is to integrate recent PEFC technology developments at LANL with stack development activities in industry, in order to fabricate and demonstrate a manufacturable, low-cost/high-performance hydrogen/air fuel cell stack operating at

ambient inlet pressures for generation of electric power from hydrogen. The stack is to be based on MEAs (patents issued) and non-machined stainless steel hardware (patent allowed for the pressurized embodiment), developed at LANL. A co-operative research and development agreement (CRADA) between LANL and an industrial partner includes tasks ranging from the exchange, testing and optimization of membrane-electrode assemblies of larger areas, through development and demonstration of manufacturable flow-fields, electrode backing and bipolar plate components, to testing of stacks at the 3-5 cell level and finally, stack demonstration at the 4-5 kW level.

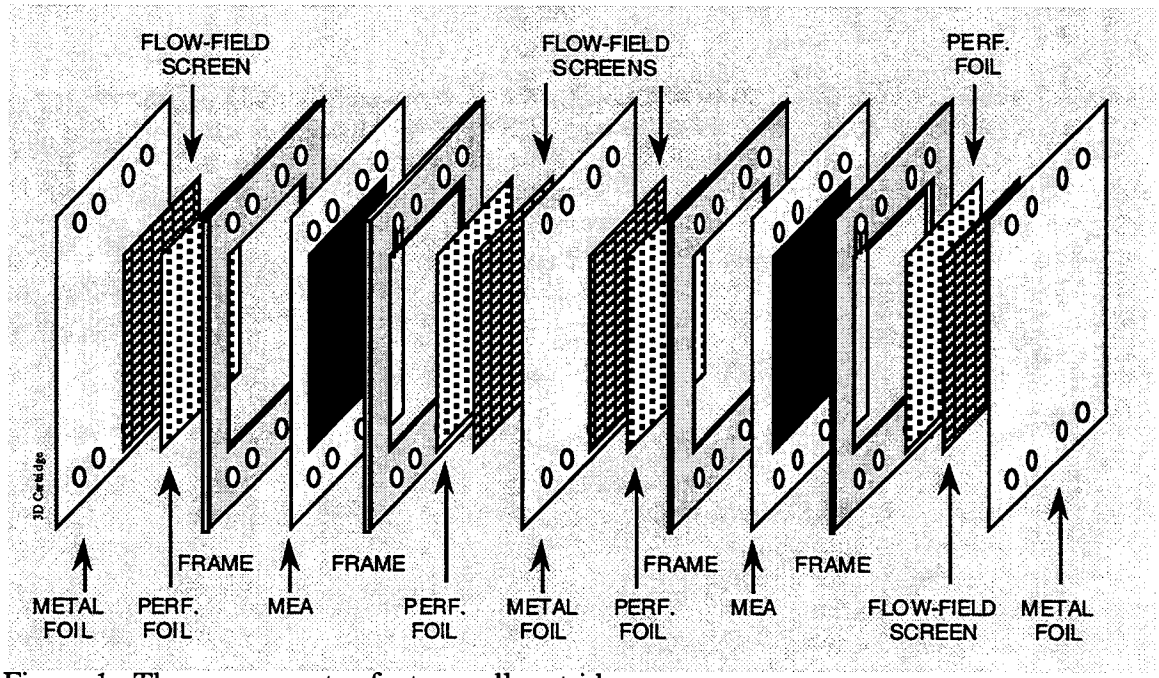


Figure 1. The components of a two-cell cartridge.

## Past Results

Past results were oriented around a stack designed for pressurized operation utilizing low-cost 316 stainless steel wire screens and foils as gas flow-fields/bipolar plates. A 100 $cm^2$ single cell was operated for 2000 hours of continuous testing using such 316 stainless steel screen/foil hardware. There was no significant drop in cell performance. Specifically, no rise was recorded in the high frequency resistance after 2000 hours of continuous operation. Tests with similar stainless steel hardware were repeated by industry under ambient pressure conditions. We developed a two-cell "cartridge" configuration, the components of which are shown in Figure 1. Relatively coarse wire screens are used as the flow-fields and, in a new development, thin perforated foils are used instead of the original fine screens to prevent the membrane electrode assembly from impalement by the flow-field screen. Thin metal foils function as the gas-tight separators between the flow-field elements and plastic frames provide sealing surfaces and manifolding for the reactant supply to the individual flow-fields through channels formed in the corners. The "corner-to-corner" flow that was thus attained provided effective reactant distribution, as indicated by the good performances attained with only two times stoichiometric air-flow.

Figure 2 provides a possible explanation of the success of the corner-to-corner flow configuration. Since reactant flow can not proceed in a diagonal direction between neighboring "elements" of the square weave wire screen, it must still assume a staircase path to proceed directly form one opposing corner to the other. The effective length of this

staircase path is the same as straight down and straight across or of any progressive path. Consequently, the flow distribution to all areas is relatively uniform.

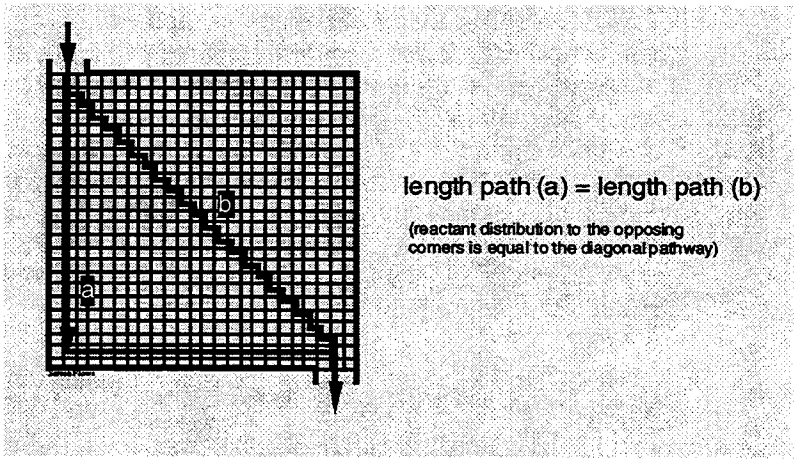


Figure 2. The corner-to-corner reactant flow scheme.

One of the developments not reported last year was the replacement of the fine screen used to protect the MEA from the flow-field screen with a fine perforated foil. One of the difficulties with the fine screen shown in Figure 3 was that water tended to collect within the grids unless the screens were rendered hydrophobic by heat-treatment with PTFE, and then it was necessary to abrade the sides placed against the carbon-cloth backings of the MEAs for conductivity. Despite all this, some stability problems still occurred. Our solution was to replace the fine screens with thin perforated foils that were about 50% open area with 1 mm diameter staggered perforations. Under compression, the relatively soft carbon cloth backing deformed somewhat into the openings in the foil and were immediately adjacent to but still protected from the flow-field screen. As such, no "cells" were available for water entrapment and stability was attained without requiring any treatments. The perforated foils in this case are prepared by photolithography techniques utilizing acid-etching so large scale production can possibly be competitive with standard mechanical perforation plus final shaping.

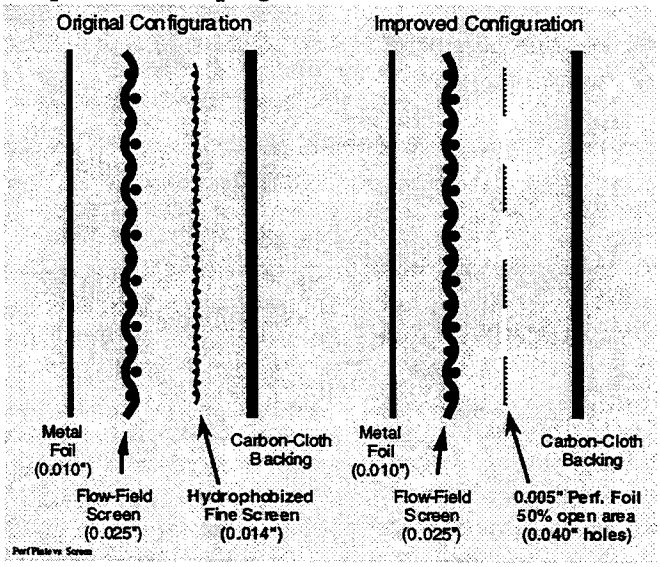


Figure 3. Comparison of cell configurations using either treated fine screens or fine perforated foils.

Several four cell stacks were assembled using the perforated foils and two 2-cell cartridges sandwiched around a cooling plate. Some difficulties were encountered first with shearing of the membranes in the MEAs during assembly as the components around the periphery settled at a different rate than the compressible components in the active area. This was solved by overlapping some of the components in a manner that protected the vulnerable region of the membrane. Additional difficulties were obtained using the water-cooled cooling plate because the cells adjacent the plate dropped in performance significantly whenever the cooling pump switched on. Similar difficulties have been reported in other stack designs, but were probably greatly exacerbated with our thin foil/low thermal mass design. Four-cell stacks that provided individual cell performances close to single cells or double cell cartridges were accomplished by carefully moderating the coolant supply such that the temperature differentials were minimal.

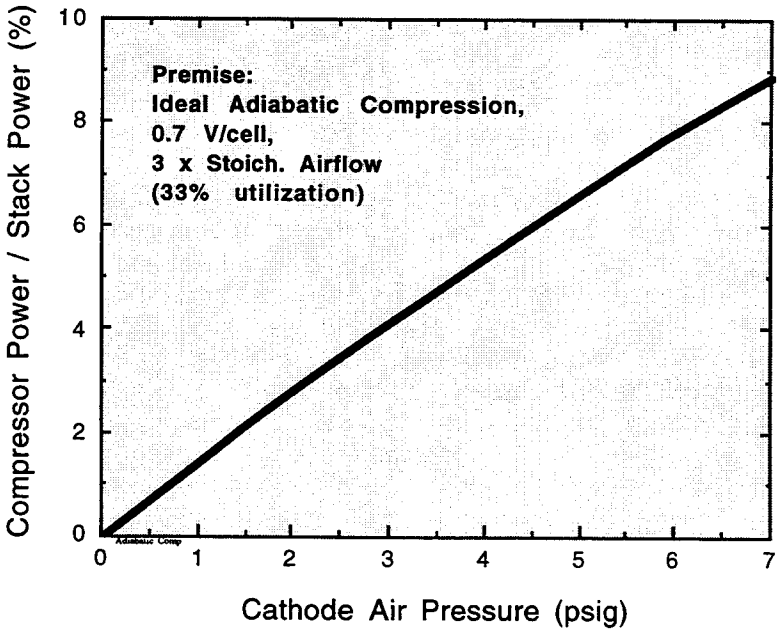


Figure 4. Parasitic power requirements for an ideal adiabatic compressor as a function of air-side pressure.

## Current Year Accomplishments/Status

Efforts this year have been redirected to an ambient pressure stack and the cell size has been scaled up to active area of 300 $cm^2$ for the target 4 kW stack. This redirection originally resulted from a programmatic need to coordinate testing with a mobile system requiring ambient pressure operation, however, the advantages inherent to ambient air operation are also beneficial for some stationary applications. The primary advantage is the lower parasitic power requirements with near-ambient pressure cathode operation compared to pressurized operation. For example, the 30 psig pressurized fuel cell system operating on hydrogen demonstrated by one major fuel cell developer requires about 20% of the electrical power produced to operate the system auxiliaries. The largest power loss is the air compressor even though the system runs at an efficient two times stoichiometric flow. The situation would be even worse except that an expander is used on the air effluent to recover as much of the PV work as possible. This compressor/expander package is becoming a major technical and cost challenge in fuel cell system design. Neither turbine nor positive displacement (e.g. rotary scroll) compressor/expander systems promise to be

particularly efficient (ca. 50% each step) or inexpensive. Thus, substantial complexity, cost and power savings can conceivably be realized by operating at ambient pressure on the air side. Others, such as the Shatz Energy Research Center and International Fuel Cells have developed near ambient pressure systems, and we are correspondingly developing non-machined fuel cell hardware based on 316 stainless steel as before, but now the flow-field design must be amenable to ambient pressure operation. As such, we have needed to evolve our earlier pressurized foil and screen design such that the reactant pressure drop on the air side is extremely low. We are targeting pressure drops of about 1" $H_2O$ or less (there are about 28" $H_2O$ per psi). The desire for such low pressure drops can be understood by considering Figure 4. This figure depicts the ideal adiabatic power requirements as a percentage of total stack power to compress air at three times stoichiometric flow to the corresponding pressures of the abscissa. If, for example, a pressure of only two psig was required to push the appropriate amount of air through a fuel cell stack and water-recovery condenser, then about 3% of the stack power would ideally be required for the 2 psig compression. In reality, a bladed compressor would be only about 50% efficient, so already 6% of the stack power is required just for a seemingly modest amount of pressure. Hence, we are attempting to keep the total pressure required below about 3" $H_2O$.

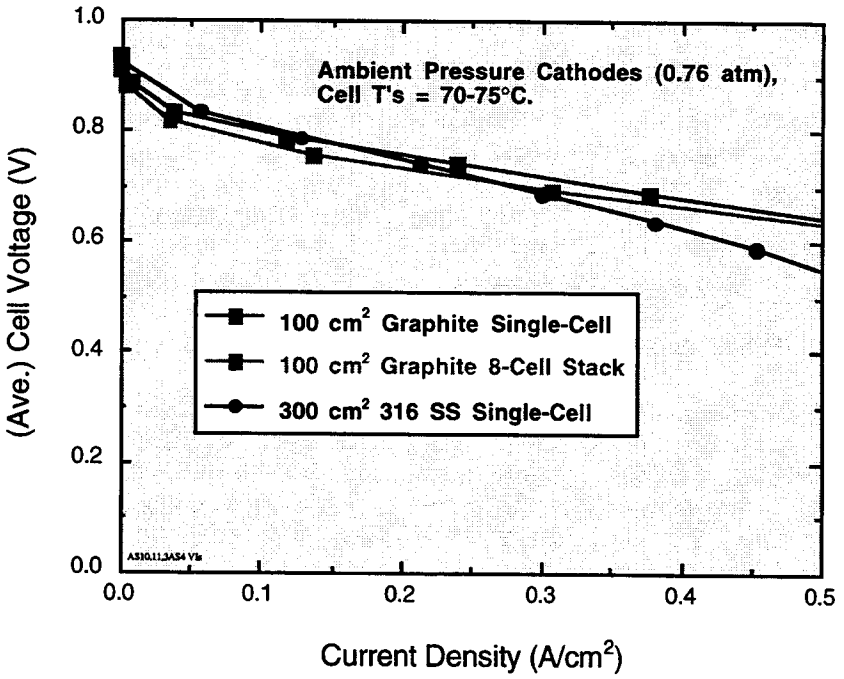


Figure 5. Polarization curves comparing the ambient pressure performance of the new 300 $cm^2$ metal hardware design to smaller, optimized graphite cells and stacks.

In addition to very low pressure drops, the new metal hardware configuration provides a pitch per unit cell of just 2.2 mm (including cooling). With a current density of 0.3 A/$cm^2$ at 0.7V (57% energy conversion efficiency hydrogen-to-electricity (DC)), the "active" volumetric power density approaches 1 kW/liter, which compares favorably with pressurized systems. Figure 5 depicts a polarization curve for a 300 $cm^2$ metal hardware single cell of the new design compared to results we obtained previously with a 100 $cm^2$ active area ambient pressure system that used relatively thick graphite plates. As can be observed, we nearly replicate the performance of the smaller cells/stack at 0.7 V although the larger cells drop off more quickly which may reflect less uniform reactant distribution in

a relatively non-optimized configuration. Note that these curves are at an ambient pressure of 0.76 atm because our laboratory is at an altitude of 7300 ft (2250 m). Between the water vapor pressure and the diminished total pressure, operation at sea level would increase the oxygen partial pressure in the plenum about 60%, so considerably higher performances may be attained under conditions that are, in most cases, more relevant.

We have had some difficulties identifying blowers that provide sufficient pressures and flowrates at reasonable power levels. Most of the low flowrate commercial DC blowers are inadequate because they are invariably designed with forward swept blades for maximum airflow at zero pressure head and so are particularly inefficient at even the modest 2" $H_2O$ pressure. As a compromise, we are using a somewhat oversized backward swept controllable AC blower, that is still sufficiently efficient (at 2" $H_2O$ and about 20 cfm for the 4 kW stack) that the parasitic power requirement should be comfortably less than 2% of the stack power.

Currently, the other significant parasitic power draws are for a hydrogen recirculation system and for the fan for the air effluent condenser. The former is required because in a dead-ended hydrogen feed stack the hydrogen feed tends to become humidified within the cell but condensate is left behind in the flow-field as the hydrogen reacts away. If the condensate collection is excessive, it blocks hydrogen access and cell performance suffers. One approach, employed in the hydrogen fueled Ballard bus, is to use a venturi ejector on the hydrogen supply line to instill a small vacuum at the stack effluent such that some circulation is achieved. While this doesn't consume any power, it is difficult and expensive to implement on the 4 kW scale. In the 400 W graphite stack depicted in Figure 5, we were able to use a small diaphragm recirculation pump that consumed less than 2 W (or less than 0.5% of the stack power). Unfortunately, the pump power requirement does not scale to the 4 kW level as efficiently. The best recirculation pump that we have thus far found would require about 100 W or 2.5% of the stack power. As such, we are working on a simple hydrogen recirculation system that uses the PV work available in the pressurized hydrogen supply, as does Ballard, to instill recirculation in the stack. The power requirements will hopefully be less than several watts.

The other significant power draw is the fan for the water condenser. An ambient pressure system running at, for example, 70° C and several times stoichiometric airflow, will operate in a net water deficit because more water will be removed as vapor than will be formed in the cathode reaction. In order to maintain a positive water balance, it is necessary to recover a significant fraction of the water vapor. We initially experimented with a modified automobile radiator but the power required for the cooling fan was on the order of 3% of the total power and the pressure drop through the radiator for the cathode effluent was uncomfortably high. One of the reasons for the high fan power requirement was that an inordinate amount of cooling air was required to achieve the required cooling. A conventional radiator essentially consists of primary flow tubes with numerous cooling strips or fins in order to increase the heat transfer surface area several fold. Unfortunately, the operating temperature of the fuel cell condenser may only be 60° C whereas an internal combustion engine radiator operates at a significantly higher temperature. As such, the fin efficiencies are particularly poor with the modest temperature differentials and the available surface area is not effectively utilized. Correspondingly, we have assembled a lightweight, low-pressure drop condenser that maximizes the surface area of the flow channels. While we have not yet fully characterized the heat transfer coefficients, etc., it appears that we should be able to need only about 1.5% of the power to run the cooling fan.

Taking all of the above into account, the parasitic power levels for this evolving nominal 4 kW system are favorably projected to be:

| | |
|---|---|
| Blower: | < 2 % |
| New $H_2$ recirculation system: | < 0.1 % |
| Water pump | < 0.1 % |
| Fan for new condenser design | 1.5 % |
| **Total Parasitic Power Loss** | **< 3.7 %** |

The electronics for monitoring and controlling such a system are not included but the power consumption of the microprocessors and digital interface electronics are nearly negligible compared to the other factors. Motor controller inefficiencies are already included in the blower value and the others may be simple off-on systems. In any case, the ability to operate with less than 5% parasitic power losses may make such systems competitive with more sophisticated efforts, notwithstanding the cost and complexity advantages. For example, a pressurized system with 20% parasitic power losses would need to operate at 0.83 V/cell in order to provide the same overall efficiency as the ambient pressure system with 5% parasitic power losses operating at 0.70 V/cell. In this comparison, equivalent current densities provide equivalent net power densities. As such, the pressurized system would also need to achieve 300 mA/cm$^2$ at 0.83 V to match the ambient pressure power density at 0.7 V. Even with pressurization, it would be difficult to achieve the 300 mA/cm$^2$ at 0.83 V with low platinum catalyst loadings. In order to improve the kinetics sufficiently to attain this performance, it would probably be necessary to increase the catalyst loadings by a factor of 5 to 10, which would incur a significant cost penalty.

In stationary power applications, the condenser (and fan) could conceivably be eliminated if a water supply is available at the site. This roughly 1.5% increase in efficiency would require the supply and demineralization of about 12 gallons per day of water for a 4 kW system. This trade-off may be attractive for a number of situations. Another practical consideration of stationary power applications is that the preferred fuel will eventually most likely be natural gas. Depending on the fuel processor design approach, a pressurized anode (e.g., 30 psig) may be advantageous in some cases. The general scheme that we are adopting is amenable to operation with a pressurized anode and an ambient pressure cathode. Such a combination may provide the most efficient package overall.

We are continuing investigating corrosion in cells using 316 SS components. Most of our previous testing was performed on single cells or using immersion cells. While the single cell results that we reported were very encouraging, one of the difficulties with multiple cell stacks is that higher (than single cell) voltages may occur due to shunt currents in the manifold region. Testing of the effluent water from the 4-cell pressurized screen/foil stacks on the 100 h time scale indicated that the levels of Mn, Ni, Cr, Mo and Mg were all significantly below 1 ppm and, while greater, Fe was also still below 1 ppm. Thus, it appears that any dissolution processes were relatively minor and no visible corrosion was apparent after disassembly. We have heard from others that they have experienced corrosion difficulties using 316 SS although the liquid effluents from their stacks were indicated to have pH's significantly lower than the 6 to 7 that we typically observe. Last year, we investigated corrosion rates in aggressive immersion testing using pH 2 solutions at 80°C as well as micromolar amounts of chloride ions (which are known to exacerbate corrosion). Substantial metal ion contents were observed for the hydrogen sparged solutions (e.g., up to 70 ppm for Fe), much less so for the air-sparged (all metal ions less than 1 ppm), and a chloride ion effect was not evident. Given that difficulties were apparent at pH's of two, this year we extended the immersion testing to cover pH's of 2, 3, 4, 5 and DI water, as well as longer immersion times (500 vs. 250 h), and more samples for better statistics. The solutions were analyzed for metal ion contents using ICP-MS or ICP-ES. They were also weighed before and after. While not particularly accurate because

of the small changes involved, the gravimetric results yielded corrosion rates less than 0.34 μm/yr for all samples.

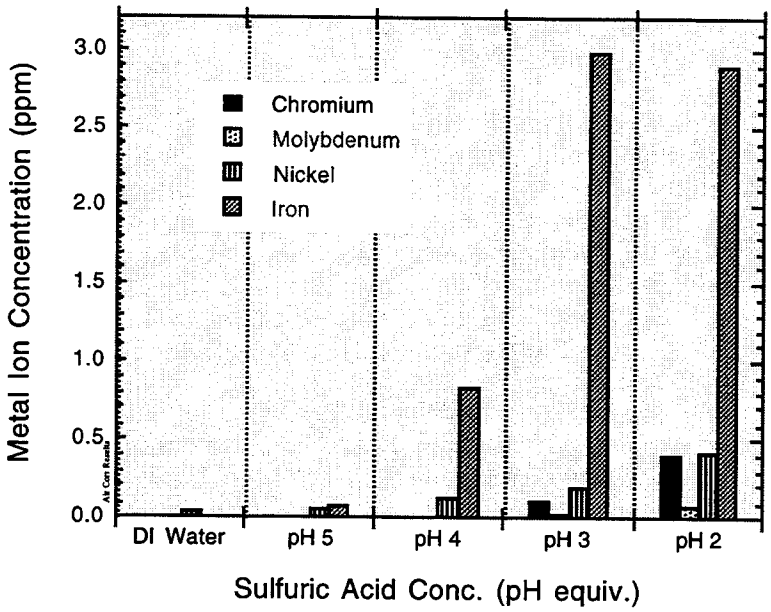


Figure 6. Metal ion contents as a function of solution acidity of the air sparged immersion solutions containing 316 SS samples.

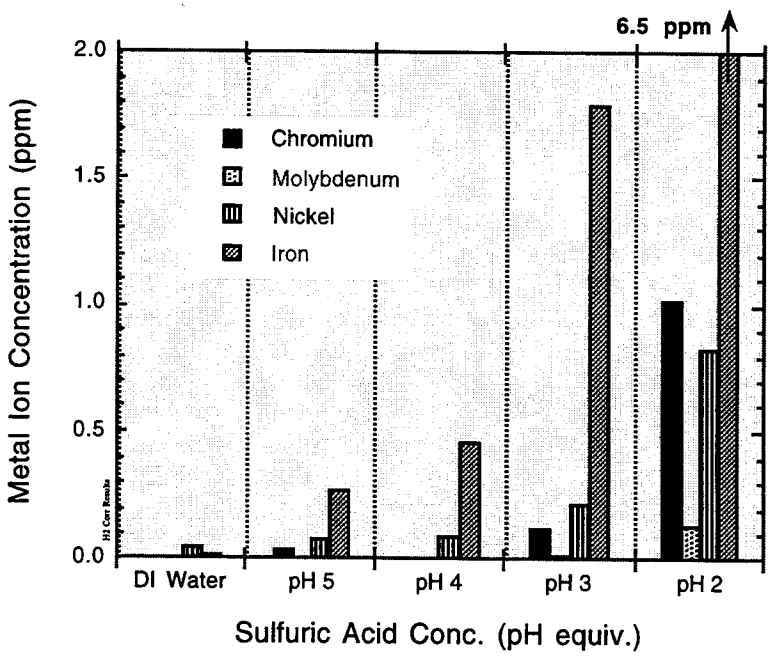


Figure 7. Metal ion contents as a function of solution acidity of the hydrogen sparged immersion solutions containing 316 SS samples.

Figure 6 depicts the average metal ion contents of the air-sparged samples and Figure 7 summarizes the results for the hydrogen sparged experiments. In both cases, the metal ion contents are near or below detection levels in DI water (pH 6 - 7) and gradually escalate

with acidity until the concentrations are several orders of magnitude higher in some cases. As before, most ion contents in the hydrogen sparged solutions are higher, which might be expected from the reduction and dissolution of the passivation layer. In general, it is clear that if abnormal liquid water acidities within the cell can be avoided there is a good possibility that long term stability can be achieved.

One of the hazards of dissolution is that the metal ions may, in some manner, make it to the ionomeric membrane and tie up functional sites effectively increasing the ionic resistivity and cell resistance. It was also considered that, in some designs, the metal hardware may be in direct contact with the membrane, which may facilitate the dissolution and uptake of metal ions. As such, in an experiment, 316 SS screen hardware was placed in direct contact with an uncatalyzed Nafion 112 membrane and the "cell" was operated at 80°C under heavily humidified $H_2$ and air with an imposed "open circuit" voltage of 0.94 V for 120 h. Afterwards, the hardware showed no visible signs of corrosion, however, the membrane was indeed discolored. Analysis of the membrane by EDAX could only detect Cu above the 304 SS background of the SEM instrument. More sensitive analysis with XRF did detect minute traces of stainless steel components such as Fe, Ni, Cr and Mn but other elements such as Cu, Zn and Ca were observed. No molybdenum (Mo), which differentiates 316 from 304 SS, was detected. If no 316 SS dissolution actually occurred, possible sources of the 304-type metal ions could conceivably have been the 304 SS humidifier system in the test station. The Cu and Zn may have come from aluminum alloy in the endplate manifold region, and Ca may come from non-ionic colloidal oxides not removed by the deionization system. Si from colloidal silicates and Al from the endplates may have been present but below the detection threshold of the XRF. In any case, the total ionic concentrations are quite small and it does not appear that the 316 SS was unduly affected by direct contact with the membrane. In retrospect, a possible weakness with this experiment was that no current was passing through the membrane in the simulated open circuit conditions, and contaminant ion inclusion has been demonstrated to be a function of current in some industrial membrane electrochemical reactors.

The effluent pH's from the above cell were about 6 from both sides. Metal against the membrane did not prompt low effluent pH's although a possible mechanism is not clear anyway. It is still somewhat of a mystery to us why the low pH effluents observed by others may occur. Possibilities are contaminants from the particular fabrication processes employed or from the materials used themselves or the reactants or water supply. Cell reversals or shunt currents may result in unusual chemistries, although again, it is not clear what mechanisms could conceivably result in acidic ionic species.

The general conclusion from the additional corrosion testing this year is that there still does not appear to be any readily evident difficulties with the use of untreated or uncoated 316 stainless steel for the fuel cell hardware, at least on the single-cell or short-stack level. The primary challenge then, will be to minimize or eliminate shunt currents in large stacks. We have naturally attempted to design our components to alleviate such occurrences, but have not yet had the opportunity to evaluate their performance under such conditions.

## Economic Evaluation

Compared with present day PEFC stack technologies, the metal flow-fields demonstrated provide very low costs. The most recent configuration could conceivably cost $2-3/kW, vs. $100/kW projected for machined graphite flow fields. This brings the total cost of fuel cell materials down to practically the cost of the MEA, which today is about $300/kW at 60% energy conversion efficiency. A present day overall cost estimate of $600/kW would

be quite acceptable, considering a stationary power generation market entry cost target of around $2000/kW (per J. Ogden & co-workers and an A.D. Little Report).

## Plans for Future Work

Milestone 1: Complete fabrication of 4 kW stack based on stainless steel hardware and operating at ambient air pressure -- July 15, 1998.
Milestone 2: Demonstrate stack system bench operation at parasitic power loss < 10% -- Sept. 30, 1998.

## Publications

1. Simon Cleghorn, Xiaoming Ren, Thomas Springer, Mahlon Wilson, Christine Zawodzinski, Thomas Zawodzinski and Shimshon Gottesfeld, "PEM Fuel Cells For Transportation And Stationary Power Generation Applications," *Int. J. Hydrogen Energy,* **22**, 1137-1144 (1997).

2. Christine Zawodzinski, Mahlon S. Wilson and Shimshon Gottesfeld, "Corrosion Testing of Stainless Steel Fuel Cell Hardware," paper submitted to The 1998 Fuel Cell Seminar, Palm Springs, CA.

3. Christine Zawodzinski, Mahlon S. Wilson and Shimshon Gottesfeld, "Metal Screen and Foil Hardware for Polymer Electrolyte Fuel Cells," abstract submitted to the Fall 1998 ECS Meeting, Boston, MA